



## Short communication

Electrochemical properties of TiO<sub>2</sub> hollow microspheres from a template-free and green wet-chemical routeBo Song<sup>a</sup>, Shengwei Liu<sup>b</sup>, Jikang Jian<sup>c</sup>, Ming Lei<sup>a</sup>, Xiaojian Wang<sup>a</sup>, Hong Li<sup>a</sup>, Jianguo Yu<sup>b</sup>, Xiaolong Chen<sup>a,\*</sup><sup>a</sup> Beijing National Laboratory for Condensed Matter Physics, Institute of Physics, Chinese Academy of Sciences, P.O. Box 603, Beijing 100080, China<sup>b</sup> State Key Laboratory of Advanced Technology for Materials Synthesis and Processing, Wuhan University of Technology, Wuhan 430070, China<sup>c</sup> Department of Physics, Xinjiang University, Urumchi 830046, China

## ARTICLE INFO

## Article history:

Received 8 October 2007

Received in revised form 25 February 2008

Accepted 27 February 2008

Available online 2 March 2008

## Keywords:

Electrochemistry  
Lithium-ion batteries  
Microspheres  
Titanium dioxide

## ABSTRACT

Electrochemical properties of TiO<sub>2</sub> hollow microspheres from a green and template-free route were investigated by charge–discharge, cyclic voltammograms, cycle performance, and high rate capacities measurements. The storage capacity of Li ions in the first discharge process was 290.3 mAh g<sup>-1</sup>. During the successive 10 cycles, the reversible capacity stayed in the range from 290 to 130 mAh g<sup>-1</sup> with a capacity fading of 8.96% per cycle. Cyclic voltammograms measurement exhibited only a pair of reduction/oxidation peaks, indicating TiO<sub>2</sub> hollow microspheres with a good crystalline quality was approached in this route.

© 2008 Elsevier B.V. All rights reserved.

## 1. Introduction

Recently, hollow inorganic micro- and nanostructure have attracted considerable attention because of their potential applications such as nanoscale chemical reactors, drug-delivery carrier, artificial cells, catalysis, and chemical storage cells [1–10]. Especially in the field of electrochemical storage [11–13] hollow structure is of great interest to chemists and materials scientists due to their large surface areas and thin walls, which could decrease the current density per unit surface area and shorten the Li-diffusion length in solid phase, respectively [11]. As a wide-bandgap semiconductor ( $E_g = 3.2$  eV), TiO<sub>2</sub> has been intensively investigated as a key material in lithium-ion batteries owing to its excellent performance in low voltage insertion and a fast insertion/extraction for Li ions [14–17]. From the view point of technological application, TiO<sub>2</sub> hollow micro- and nanospheres are suggested to be serving as the promising cathode materials for high-power lithium-ion batteries [18–25]. Until now, hollow micro- and nanospheres of TiO<sub>2</sub> have been approached by a variety of sol–gel methods [26] and removable or sacrificial templates, including hard ones such as monodispersed silica [27], carbon spheres [28–31], polymer latex film [32] or polystyrene (PS) [33–35], as well as soft ones,

for instance, emulsion droplets/micelles [4]. However, high cost and tedious manipulation procedures are often involved via the templating pathways, which limit TiO<sub>2</sub> hollow micro/nanospheres from being used in large scale. To overcome the complexity of templating methods, facile and template-free routes to TiO<sub>2</sub> hollow micro/nanospheres have been developed, based on the mechanism of Ostwald ripening, differential diffusion (Kirkendall effect), as well as self-assembly of performed building blocks [2,36,37]. However, large-scale synthesis of hollow TiO<sub>2</sub> microspheres is still a challenge, not to mention via a green pathway in which only the environmentally friendly (non-toxic and can be recycled easily) reagents are involved in the reactions [38,39]. Therefore, to develop a green, simple and economic strategy for the preparation of TiO<sub>2</sub> hollow micro/nanostructures is highly desirable, which is of considerable general interest to the materials community. But, there are very few reports describing the synthesis process from one-pot template-free method without hazardous organic solvents involved until the very recently that Yu et al. proposed a facile one-step template-free route to prepare inorganic hollow inorganic microspheres including TiO<sub>2</sub>, SnO<sub>2</sub>, etc. [30]. Although the morphologies of the TiO<sub>2</sub> hollow structures obtained by Yu et al. is not optimal compared with other routes involved organic solvents, this convenient method makes it possible to utilize the electrochemical properties of TiO<sub>2</sub> hollow spheres in large-scale. It is believed that investigation of TiO<sub>2</sub> hollow structures as electrode materials from a green and facile route will advance the development of batteries

\* Corresponding author. Tel.: +86 10 82649039; fax: +86 10 82649646.  
E-mail address: [chenx29@aphy.iphy.ac.cn](mailto:chenx29@aphy.iphy.ac.cn) (X.L. Chen).

industry. The characters of environmentally friendly were considered as absolutely necessary element in the future fabrication and application process of batteries materials. Thus, the TiO<sub>2</sub> hollow structures are deserved to investigate its potential applications in field of chemical storage. To our knowledge, the electrochemical features of TiO<sub>2</sub> hollow microspheres via template-free and green wet-chemical route have not been studied until now.

Herein, we report the electrochemical properties of TiO<sub>2</sub> hollow microspheres, which was synthesized at 180 °C from a reaction of Ti(SO<sub>4</sub>)<sub>2</sub> and NH<sub>4</sub>F, based on a localized Ostwald ripening mechanism. The as-prepared TiO<sub>2</sub> hollow microspheres exhibit improved storage capacity and cycle performance than that of TiO<sub>2</sub> powder when it is used as cathode material.

## 2. Experimental

All chemical reagents in this work were purchased from the Beijing Chemical Company, China. They were of analytical grade and used without further purification.

### 2.1. Preparation of TiO<sub>2</sub> hollow microspheres

The details of a typical experiment for the synthesis of TiO<sub>2</sub> hollow microspheres are as follows: 50 mL concentrated H<sub>2</sub>SO<sub>4</sub> were added into 100 mL distilled water to form dilute solution of H<sub>2</sub>SO<sub>4</sub>. Then, Ti(SO<sub>4</sub>)<sub>2</sub> was dissolved in the as-prepared solution to give a Ti(SO<sub>4</sub>)<sub>2</sub> concentration of 0.5 M. The obtained solution was clear and stable for 10 h at room temperature. 50 mL of NH<sub>4</sub>F (0.5 M) solution were added to the as-prepared acidic Ti(SO<sub>4</sub>)<sub>2</sub> solution under vigorous stirring for 10 min. The mixed solution was transferred to a Teflon-lined stainless autoclave (100 mL capacity), which was kept at 180 °C for 9 h and then cooled to room temperature naturally. The white precipitate was washed with distilled water and absolute alcohol for several times to remove the possible residues and then dried at 80 °C for 6 h under vacuum.

### 2.2. Sample characterization

Samples for transmission electron microscopy (TEM) and selected area electron diffraction (SAED) analysis were deposited on carbon-coated 3 mm diameter, copper electron microscope grids and dried in air. TEM analysis was performed in bright-field mode using a JEOL 1200 EX at 120 keV. Scanning electron microscopy (SEM) observations were performed on the FEI XL 30 S-FEG. Energy-dispersive X-ray (EDX) analysis was performed on the Oxford energy-dispersive X-ray analysis system linked to the SEM. Phase analysis were carried out using X-ray diffraction (XRD) on a MAC-M18XHF (Cu Kα<sub>1</sub>/α<sub>2</sub>, λ = 1.5418 Å, 50 kV, 200 mA). Raman measurements were performed on multichannel modular triple Raman system JY-T64000 (Jobin-Yvon) using 532 nm line (2.33 eV) as the excitation source.

### 2.3. Electrochemical measurements

The electrochemical properties of the TiO<sub>2</sub> hollow microspheres as a cathode used in rechargeable lithium-ion batteries were measured at room temperature. The working electrodes were fabricated by compressing the mixture of 80 wt.% active materials (TiO<sub>2</sub> hollow microspheres), 10 wt.% conductivity agent (carbon black, CB), and 10 wt.% binder (polyvinylidene fluoride, PVDF) dissolved in *N*-methylpyrrolidone onto a copper foil. Lithium metal foil was cut as a disk of 15 mm in diameter and used as the counter and reference electrodes. The electrolyte was 1 M LiPF<sub>6</sub> dissolved in a mixture of ethylene carbonate (EC) and diethyl carbonate (DEC) with the volume ratio of EC/DEC = 1:1. The assembly process of cell was carried

out in an argon-filled glove box (MECAPLEX, Switzerland) with the content of O<sub>2</sub> and H<sub>2</sub>O less than 3 ppm.

## 3. Results and discussion

Fig. 1A shows a representative field-emission scanning electron microscopy (FE-SEM) image of the as-prepared samples and typical morphologies of sphere-like structures were observed in this panoramic view. From high-magnification SEM images (Fig. 1B and C), it is apparent that the obtained products are interconnected hollow microspheres with a size from 800 to 1500 nm and the shell thickness of about 90–100 nm. EDX pattern (Fig. 1C, inset) shows the element composition of hollow microspheres agreeing well with that of titanium dioxide. The dark contrast in TEM images (Fig. 1D and E) further confirm the obtained products are indeed hollow structures. Especially, in Fig. 1D, one can see distinctly that three microspheres are interconnected with each other. The corresponding ring-like SAED pattern (Fig. 1D, inset) indicate the microstructures are polycrystalline and the diffraction rings from inside to outside can be indexed as (1 0 1), (0 0 4), (2 0 0), (1 0 5), and (2 1 1) planes of anatase TiO<sub>2</sub>. The presence of nanoparticles can be seen clearly in Fig. 1B and C. High-magnification SEM images (Figs. 2 and 3) show the hollow microspheres are constructed by lots of nanoparticles as the building blocks with a size distributed from 20 to 30 nm.

All the diffractions peaks in XRD pattern of the obtained TiO<sub>2</sub> hollow microspheres (Fig. 4) could be indexed well based on a tetragonal anatase phase and the lattice parameters are calculated to be  $a = 3.7858(9) \text{ \AA}$  and  $c = 9.5006(6) \text{ \AA}$ , which are in good agreement with ICDD-PDF: 65-5714 (space group  $I4_1/amd$ , number 141). XRD peaks due to other phases were not detected under the X-ray diffractometer's resolution, which undisputedly suggested that the highly pure crystalline TiO<sub>2</sub> was synthesized. From XRD results, the crystallite size can be estimated from broadening of the (1 0 1) peak by Scherrer equation [40]:

$$D = \frac{k\lambda}{(\beta \cos \theta)} \quad (1)$$

where  $D$  is the crystallite size,  $\lambda$  is the wavelength of X-ray radiation (Cu Kα<sub>1</sub>/α<sub>2</sub> radiation = 1.5418 Å),  $k$  is a constant and usually taken as 0.89,  $\beta$  is the full width at half maximum (FWHM), after subtraction of equipment broadening, and  $\theta$  is the Bragg angle of peak. From XRD results, the average sizes of the building blocks are estimated to be for about 22 nm, which is consistent well with previous SEM results. Raman spectrum of as-prepared TiO<sub>2</sub> hollow microspheres obtained at room temperature is shown in Fig. 5. The fundamental Raman scattering peaks for TiO<sub>2</sub> hollow microspheres were observed at 144, 197, 395, 515, and 636 cm<sup>-1</sup>. The peaks at 144, 197, and 636 cm<sup>-1</sup> correspond to the E<sub>g</sub> vibration mode. The bands at 395 and 515 cm<sup>-1</sup> can be assigned as B<sub>1g</sub> and (A<sub>1g</sub>, B<sub>2g</sub>) modes, respectively. All the peaks except the 515 cm<sup>-1</sup> exhibit distinct low frequency shift in contrast with TiO<sub>2</sub> micropowder (not given here). The downward shift of Raman vibration modes could be attributed to the phonon confinement effect in low dimensional materials [41].

All the discharging and charging measurements of Li-ion battery with TiO<sub>2</sub> hollow microspheres as cathode materials were performed at room temperature. In the galvanostatic voltage profiles (Fig. 6A), the TiO<sub>2</sub> hollow microspheres show a high initial discharge capacity of 290.3 mAh g<sup>-1</sup>, while the initial coulombic efficiency was up to 70.34% in the potential range from 1.0 to 4.0 V. Note that the initial discharge capacity (290.3 mAh g<sup>-1</sup>) of the as-prepared TiO<sub>2</sub> hollow microspheres is 48.28, 20.69% larger than that of commercial TiO<sub>2</sub> powder and TiO<sub>2</sub>(B) nanowires, respectively [19,21]. The carbon black and/or electrolyte decomposition

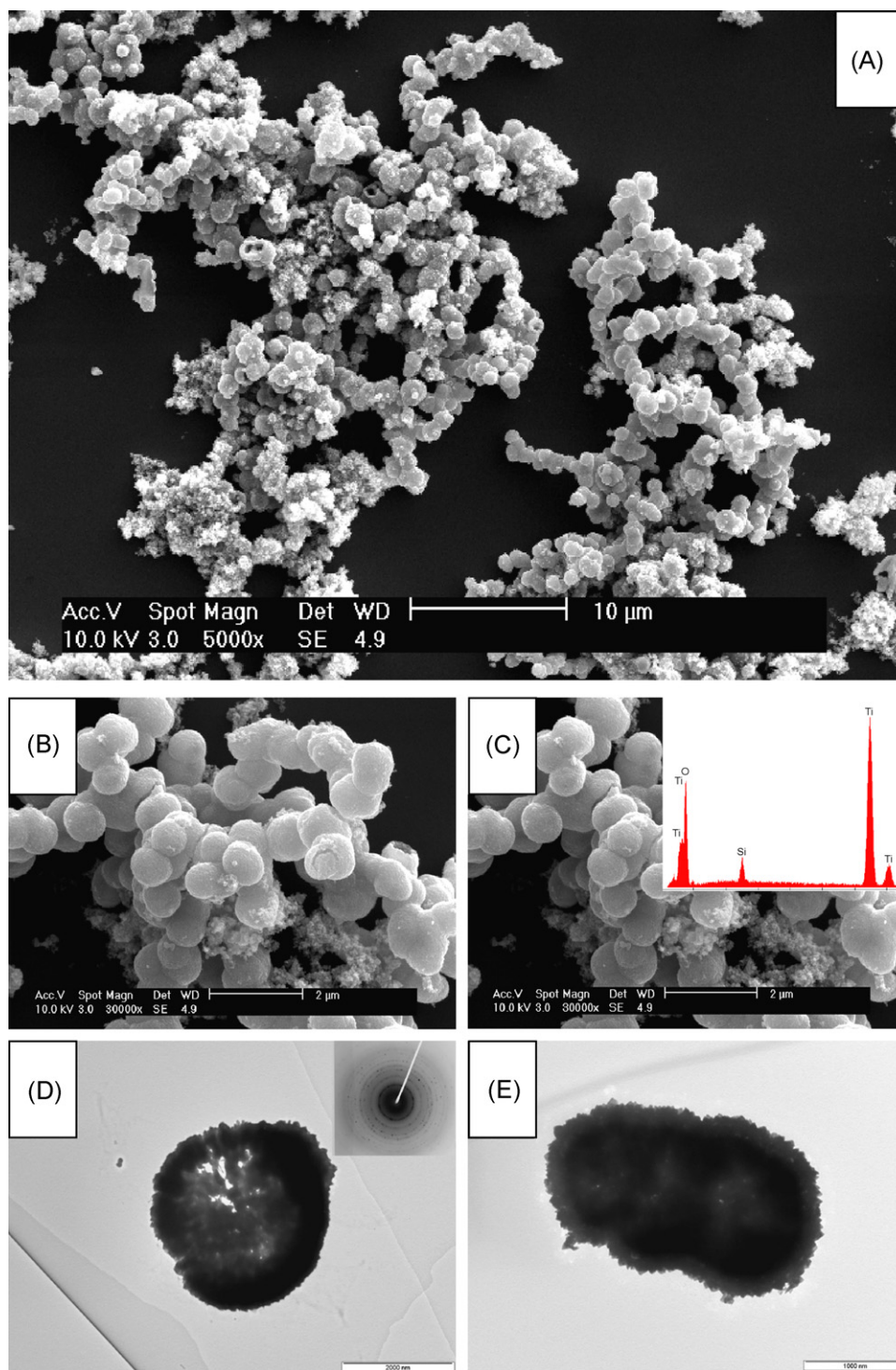


**Fig. 1.** SEM image (A) of the typical  $\text{TiO}_2$  hollow microspheres prepared at  $180^\circ\text{C}$  for 100 h. (B, C) High magnification SEM images of the  $\text{TiO}_2$  hollow microspheres. Inset (B) shows the EDX pattern of the products. (D, E) TEM images of  $\text{TiO}_2$  hollow microspheres. Inset (D) is the corresponding SAED pattern of the products.

in the as-prepared  $\text{TiO}_2$  hollow microspheres may also contribute to the storage but their capabilities are limited [42]. Thus, it is believed that the improved capacity for lithium storage of obtained samples should be attributed to the unique structure of hollow microspheres in which the diffusion distances of the solid-state lithium ion were reduced. To probe the electrochemical behavior of  $\text{TiO}_2$  hollow microspheres during the cycles, cyclic voltammograms (CV) were carried out at a scan rate of  $0.1\text{ mV s}^{-1}$  and are presented in Fig. 6B. The obtained CV profiles show an apparent

pair of cathodic/anodic peaks, located at 2.06 and 1.69 eV (vs.  $\text{Li}^+/\text{Li}$ ), respectively. These reduction/oxidation peaks can be described by two chemical processes (Eqs. (2) and (3)), which further confirm the formation of anatase  $\text{TiO}_2$  hollow microspheres in XRD [43,44].



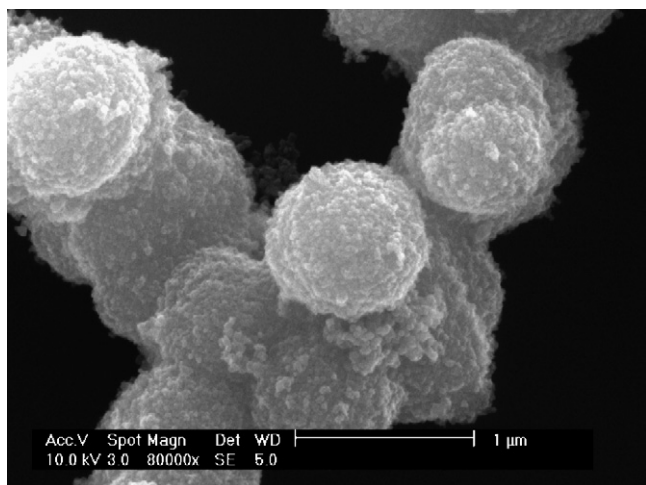


Fig. 2. High-magnification SEM image of the TiO<sub>2</sub> hollow microspheres.

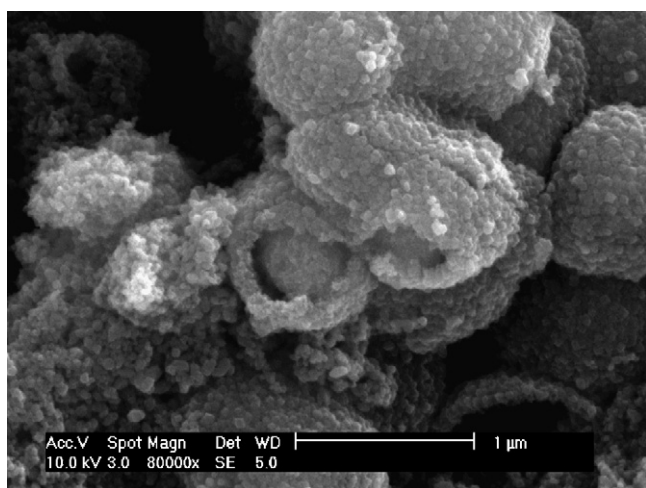


Fig. 3. High-magnification SEM image of the cracked TiO<sub>2</sub> hollow microspheres.

CV curve A is the first scan and B is the scan after one cycle. From Fig. 6B, one can see that electrochemical properties of the as-prepared TiO<sub>2</sub> hollow microspheres are quite different with that of TiO<sub>2</sub>(B) nanowires or TiO<sub>2</sub> nanotubes as reported previously

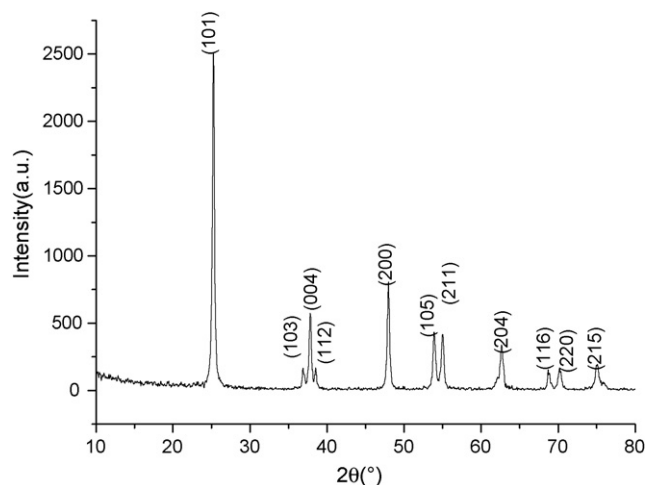


Fig. 4. XRD pattern of TiO<sub>2</sub> hollow microspheres.

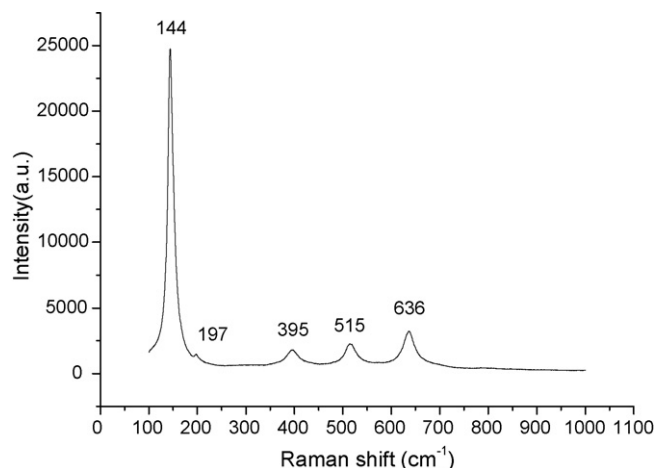
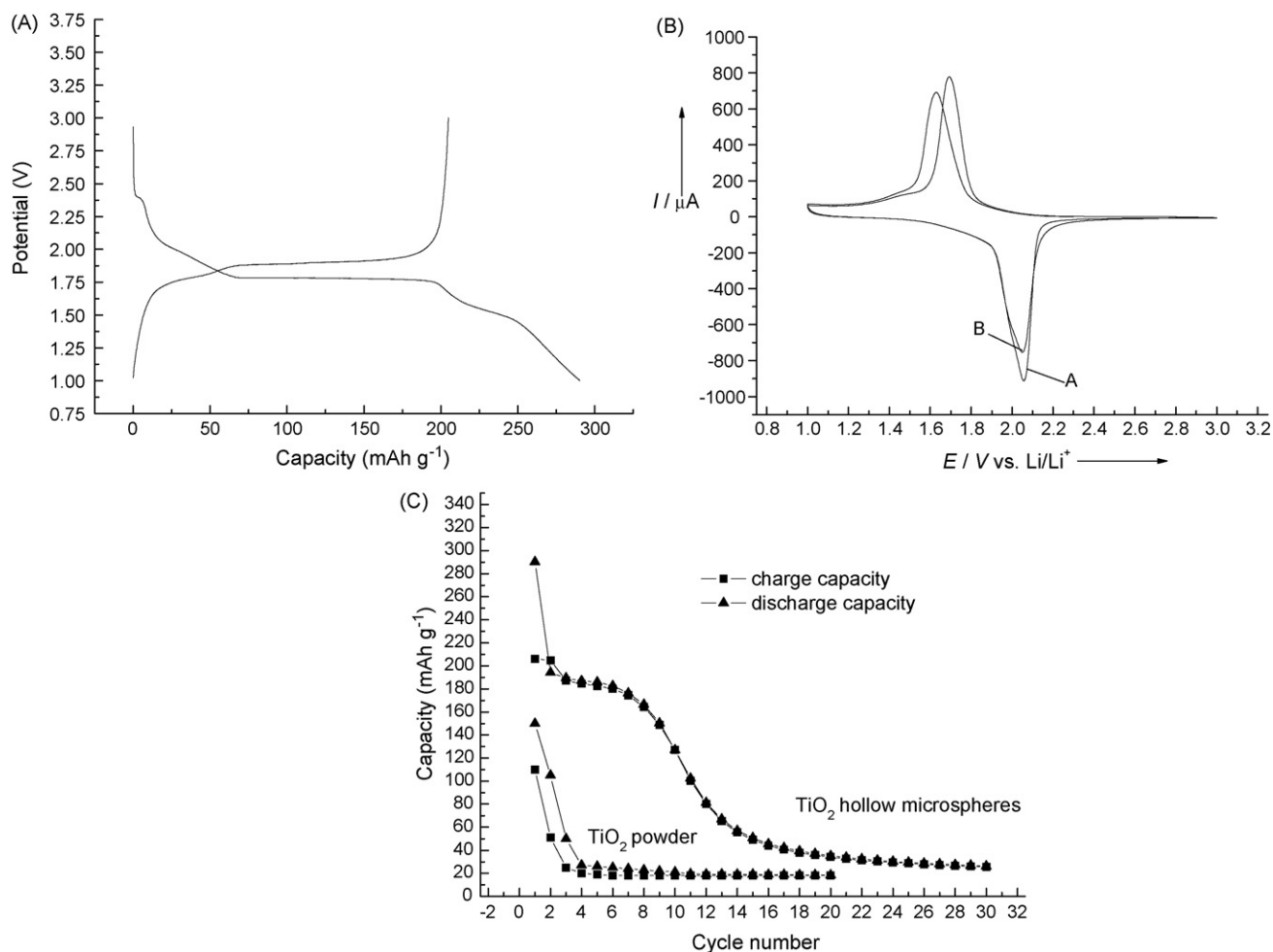


Fig. 5. Room-temperature Raman spectrum of TiO<sub>2</sub> hollow microspheres.

[18,21]. For instance, the CV characteristics showed a larger irreversible capacity and relatively much difference between the first and second cycles in TiO<sub>2</sub> hollow microspheres than that of TiO<sub>2</sub>(B) nanowires. The processes of lithium insertion and/or extraction which distort the connection between TiO<sub>6</sub> octahedra in anatase may contribute for this characteristic [20]. By contrast with TiO<sub>2</sub>(B) nanowires or TiO<sub>2</sub> nanotubes in which abundant surface imperfections such as vacancies or voids will result in surface structural changes, CV of the as-prepared TiO<sub>2</sub> hollow microspheres exhibit only a pair of reduction/oxidation peaks, indicating a good crystalline quality of products was approached by this convenient route. The variation of charge and discharge capacities against the cycle number, for TiO<sub>2</sub> hollow microspheres and TiO<sub>2</sub> powder as cathode materials under the same tested conditions, is shown Fig. 6C. To prevent the possible electrolyte reduction, the potentials was confined to larger than 1V in the measurement process. Fig. 6C shows a significant drop of irreversible capacity in the first discharge and charge process, and similar phenomenon were also observed in TiO<sub>2</sub>(B) nanowires [21] anatase [19] and rutile [17], which are not fully understood up to date. The irreversible capacity loss in this study could be attributed to irreversibly inserted lithium. In the process of successive 10 cycles, the reversible capacity for TiO<sub>2</sub> hollow microspheres stays in the range from 290 to 130 mAh g<sup>-1</sup> with a capacity fading of 8.96% per cycle larger than that of TiO<sub>2</sub>(B) nanowires and nanotubes, showing a poor electronic conductivity of the products [18,21]. This may origin from the relatively large structure strain in obtained hollow structure during repeated lithium insertion and extraction processes. Herein, TiO<sub>2</sub> hollow microspheres exhibit improved cycling performances than TiO<sub>2</sub> powder due to the both great surfaces (83 m<sup>2</sup> g<sup>-1</sup>) [39] and interesting hollow structures which could provide more insertion locations and reduce the diffusion distance of lithium ion, respectively. However, the poor cycle stability of the as-prepared TiO<sub>2</sub> hollow microspheres restricts their potential applications to substitute commercial carbon as negative electrode materials in large scale at the present state. Based on available experimental results, electrochemical properties of TiO<sub>2</sub> hollow microspheres are believed to be further improved by reducing the size of hollow cavity to nanometer-sized, which are favorable in reducing the diffusion distance of lithium ion, and result in a much higher efficiency in the intercalation and extraction processes. Generally speaking, TiO<sub>2</sub> is of considerable interests to researchers due to good safety, relatively low potential and environmental friendly of lithium batteries using it as cathode materials. In such a case, high-rate cycling behavior is one of the most important characteristics



**Fig. 6.** (A) The curves in the first discharge charge process of TiO<sub>2</sub> hollow microspheres. (B) Cyclic voltammograms of TiO<sub>2</sub> hollow microspheres obtained at a scan rate of 0.1 mV s<sup>-1</sup>. The first scan is indicated by curve A and second cycle by curve B. (C) Variation of charge (■) and discharge (▲) capacities versus cycle number for TiO<sub>2</sub> hollow microspheres and commercial TiO<sub>2</sub> powder between voltage limits of 1 and 3 V.

for a lithium ion battery. High-rate capacities of the battery using as-prepared TiO<sub>2</sub> hollow microspheres as cathode are measured at different current density as shown in Fig. 7. The cell was first cycled at the current density of 0.33 mA cm<sup>-2</sup> and after five cycles, the current density was increased to 0.66 mA cm<sup>-2</sup>. A discharge capacity of around 138.73 mAh g<sup>-1</sup> was obtained at the current density of 0.66 mA cm<sup>-2</sup> after five cycles; this value decreased to about 19.80 mAh g<sup>-1</sup> at the current density of 1.31 mA cm<sup>-2</sup> after five cycles, and finally 8.98 mAh g<sup>-1</sup> at the current density of 2.63 mA cm<sup>-2</sup> after five cycles. Here, the poor electronic conductivity of TiO<sub>2</sub> hollow microspheres inhibit the rate capability, as has been obtained in the case of rutile [17] and LiFePO<sub>4</sub> materials [45,46].

After the electrochemical investigation, the morphologies of TiO<sub>2</sub> hollow microspheres were reinvestigated by TEM and SEM. These results showed the structures of hollow microspheres remained unchanged. The formation of TiO<sub>2</sub> hollow microstructures will make the surface-to-volume ratio much higher and shorten the diffusion length for Li<sup>+</sup>, which contributes to the improvements of both reversible capacity and cycling performances. If the stresses associated with the volume changes were relieved during the processes of intercalation/extraction lithium, TiO<sub>2</sub> hollow structures from this facile and green route will exhibit better kinetic characteristics and higher value of charge/discharge capacity.

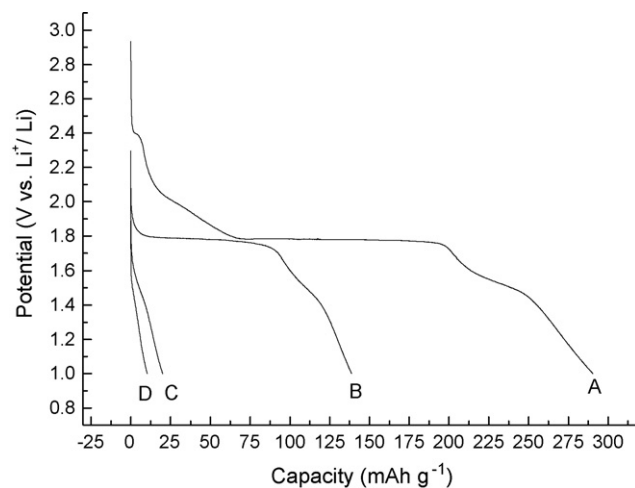


**Fig. 7.** The discharge curve of the TiO<sub>2</sub> hollow microspheres electrodes at different current density with 0.33 mA cm<sup>-2</sup> (A), 0.66 mA cm<sup>-2</sup> (B), 1.31 mA cm<sup>-2</sup> (C), and 2.63 mA cm<sup>-2</sup> (D), respectively.

In summary, we report the electrochemical properties of TiO<sub>2</sub> hollow microspheres from a green and template-free route. The storage capacity of Li ions in the first discharge process was 290.3 mAh g<sup>-1</sup>. During the successive 10 cycles, the reversible

capacity stayed in the range from 290 to 130 mAh g<sup>-1</sup> with a capacity fading of 8.96% per cycle. Cyclic voltammograms exhibited only a pair of reduction/oxidation peaks, indicating TiO<sub>2</sub> hollow microspheres with a good crystalline quality was approached. The improved electrochemical properties were mainly attributed to the unique structure of the TiO<sub>2</sub> hollow microspheres in which the diffusion distances of the solid-state lithium ion were reduced.

### Acknowledgements

This work is financially supported by National Natural Science Foundation of China (Grant Nos. 50372081, 50502039, 20473059 and 50502039), the "973" Project under the Grant No. 513270406, the Hundred Talents Project of the Chinese Academy of Sciences, Program for Changjiang Scholars and Innovative Research Team in University (PCSIRT; Grant IRT0547) and 2008 Ludo Frevel Crystallography Scholarship Award (The International Centre for Diffraction Data, ICDD, USA).

### References

- [1] F. Caruso, R.A. Caruso, H. Mohwald, *Science* 282 (1998) 1111.
- [2] Y.D. Yin, R.M. Rioux, C.K. Erdonmez, S. Hughes, G.A. Somorjai, A.P. Alivisatos, *Science* 304 (2004) 711.
- [3] H.P. Liang, H.M. Zhang, J.S. Hu, Y.G. Guo, L.J. Wan, C.L. Bai, *Angew. Chem. Int. Ed.* 43 (2004) 1540.
- [4] C.I. Zoldesi, A. Imhof, *Adv. Mater.* 17 (2005) 924.
- [5] Q. Liu, H. Liu, M. Han, J. Zhu, Y. Liang, Z. Xu, Y. Song, *Adv. Mater.* 17 (2005) 1995.
- [6] Q. Peng, Y. Dong, Y. Li, *Angew. Chem. Int. Ed.* 42 (2003) 3027.
- [7] Y. Zhu, J. Shi, W. Shen, X. Dong, J. Feng, M. Ruan, Y. Li, *Angew. Chem. Int. Ed.* 44 (2005) 5083.
- [8] M. Yang, J. Ma, C. Zhang, Z. Yang, Y. Lu, *Angew. Chem. Int. Ed.* 44 (2005) 6727.
- [9] S.W. Kim, M. Kim, W.Y. Lee, T. Hyeon, *J. Am. Chem. Soc.* 124 (2002) 7642.
- [10] H.G. Yang, H.C. Zeng, *J. Phys. Chem. B* 108 (2004) 3492.
- [11] A.M. Cao, J.S. Hu, H.P. Liang, L.J. Wan, *Angew. Chem. Int. Ed.* 44 (2005) 4391.
- [12] X.W. Lou, Y. Wang, C. Yuan, J.Y. Lee, L.A. Archer, *Adv. Mater.* 18 (2006) 2325.
- [13] C.Z. Wu, Y. Xie, L.Y. Lei, S.Q. Hu, C.Z. Ouyang, *Adv. Mater.* 18 (2006) 1727.
- [14] A. Fujishima, K. Honda, *Nature* 238 (1972) 37.
- [15] B. O'Regan, M. Grätzel, *Nature* 353 (1991) 737.
- [16] G.K. Boschloo, A. Goossens, J. Schoonman, *J. Electrochem. Soc.* 144 (1997) 1311.
- [17] Y.S. Hu, L. Kienle, Y.G. Guo, J. Maier, *Adv. Mater.* 18 (2006) 1421.
- [18] H. Zhang, G.R. Li, L.P. An, T.Y. Yan, X.P. Gao, H.Y. Zhu, *J. Phys. Chem. C* 111 (2007) 6143.
- [19] G. Sudant, E. Baudrin, D. Larcher, J.M. Tarascon, *J. Mater. Chem.* 15 (2005) 1263.
- [20] Q. Wang, Z.H. Wen, J.H. Li, *Inorg. Chem.* 45 (2005) 6944.
- [21] A.R. Armstrong, G. Armstrong, J. Canales, R. García, P.G. Bruce, *Adv. Mater.* 17 (2005) 862.
- [22] L. Kavan, M. Grätzel, J. Rathouský, A. Zukal, *J. Electrochem. Soc.* 143 (1996) 394.
- [23] H. Yamada, T. Yamatoa, I. Moriguchi, T. Kudo, *Solid State Ionics* 175 (2004) 195.
- [24] I. Moriguchi, R. Hidaka, H. Yamada, T. Kudo, *Solid State Ionics* 176 (2005) 2361.
- [25] I. Moriguchi, R. Hidaka, H. Yamada, T. Kudo, H. Murakami, N. Nakashima, *Adv. Mater.* 18 (2006) 69.
- [26] M. Iida, T. Sasaki, M. Watanabe, *Chem. Mater.* 10 (1998) 3780.
- [27] Z.B. Li, J.M. Li, Y.X. Ke, Y.G. Zhang, H.C. Zhang, F.Q. Li, J.Y. Xing, *J. Mater. Chem.* 11 (2001) 2930.
- [28] Y.D. Xia, R. Mokaya, *J. Mater. Chem.* 15 (2005) 3126.
- [29] X.M. Sun, J.F. Liu, Y.D. Li, *Chem. Eur. J.* 12 (2006) 2039.
- [30] M.B. Zheng, J.M. Cao, X. Chang, J. Wang, J.S. Liu, X.J. Ma, *Mater. Lett.* 60 (2006) 2991.
- [31] W.H. Shen, Y.F. Zhu, X.P. Dong, J.L. Gu, J.L. Shi, *Chem. Lett.* 34 (2005) 840.
- [32] Y.Z. Li, T. Kunitake, S. Fujikawa, *J. Phys. Chem. B* 110 (2006) 13000.
- [33] D.G. Shchukin, R.A. Caruso, *Chem. Mater.* 16 (2004) 2287.
- [34] R.A. Caruso, A. Susha, F. Caruso, *Chem. Mater.* 13 (2001) 400.
- [35] Z.Y. Zhong, Y.D. Yin, B. Gates, Y.N. Xia, *Adv. Mater.* 12 (2000) 206.
- [36] T. Nakashima, N. Kimizuka, *J. Am. Chem. Soc.* 125 (2003) 6386.
- [37] Y.T. Li, C.H. Song, Y.Z. Hu, Y.J. Wei, Y. Wei, *Chem. Lett.* 35 (2006) 1344.
- [38] J.G. Yu, H.T. Guo, S.A. Davis, S. Mann, *Adv. Funct. Mater.* 16 (2006) 2035.
- [39] J.G. Yu, S.W. Liu, H.G. Yu, *J. Catal.* 249 (2007) 59.
- [40] L. Gao, Q.H. Zhang, J.G. Li, *J. Mater. Chem.* 13 (2003) 154.
- [41] I.H. Campbell, P.M. Fauchet, *Solid State Commun.* 58 (1986) 739.
- [42] Z. Ying, Q. Wan, H. Cao, Z.T. Song, S.L. Feng, *Appl. Phys. Lett.* 87 (2005) 113108.
- [43] L. Kavan, M. Grätzel, S.E. Gilbert, C. Klemenz, H.J. Scheel, *J. Am. Chem. Soc.* 118 (1996) 6716.
- [44] D.V. Bavykin, J.M. Friedrich, F.C. Walsh, *Adv. Mater.* 18 (2006) 2807.
- [45] H. Huang, S.C. Yin, L.F. Nazar, *Electrochem. Solid-State Lett.* 4 (2001) A170.
- [46] M.M. Doeff, Y. Hu, F. McLarnon, R. Kostecki, *Electrochem. Solid-State Lett.* 6 (2003) A207.